Suppression of dissipation in Nb thin films with triangular antidot arrays by random removal of pinning sites

M. Kemmler,[1,*] D. Bothner,[1] K. Ilin,[2] M. Siegel,[2] R. Kleiner,[1] and D. Koelle[1]

[1]*Physikalisches Institut—Experimentalphysik II and Center for Collective Quantum Phenomena and their Applications, Universität Tübingen, Auf der Morgenstelle 14, D-72076 Tübingen, Germany*

[2]*Institut für Mikro- und Nanoelektronische Systeme, Universität Karlsruhe, Hertzstr. 16, D-76187 Karlsruhe, Germany*

(Received 10 September 2008; revised manuscript received 9 April 2009; published 8 May 2009)

The depinning current I_c versus applied magnetic field B close to the transition temperature T_c of Nb thin films with randomly diluted triangular arrays of antidots is investigated. Our experiments confirm essential features in $I_c(B)$ as predicted by Reichhardt and Olson Reichhardt [Phys. Rev. B **76**, 094512 (2007)]. We show that, by introducing disorder into periodic pinning arrays, I_c can be enhanced. In particular, for arrays with fixed density n_p of antidots, an increase in dilution P_d induces an increase in I_c and decrease of the flux-flow voltage for $B > B_p = n_p \Phi_0$.

DOI: 10.1103/PhysRevB.79.184509 PACS number(s): 74.25.Qt, 74.25.Sv, 74.78.Na

I. INTRODUCTION

The investigation of vortices in type-II superconductors in the presence of tailored pinning potential landscapes has attracted a lot of theoretical and experimental interest. On the one hand, vortices in superconductors may act as a model system in order to investigate general properties such as the dynamics and phase transitions in systems of interacting particles (e.g., colloidal suspensions,[1,2] Wigner crystals,[3] charge-density waves,[4] or various types of ratchets and Brownian motors[5–7]). On the other hand, the ability to manipulate and control the static and dynamic properties of vortices is fundamental for superconducting device applications.[8]

Modern lithography techniques allow the placement of artificial pinning sites into superconducting thin films with well-defined size, geometry, and spatial arrangement. In case of periodic arrangements, enhanced vortex pinning was found for magnetic fields, at which the vortex lattice is commensurate with the pinning array.[9–14] The enhanced pinning leads, e.g., to peaks in the critical depinning current I_c at multiples of a so-called first matching field $B_p = n_p \Phi_0$; here the density of vortices carrying one flux quantum $\Phi_0 = h/2e$ equals the density of pinning sites n_p. However, at nonmatching fields the vortex lattice is less pinned due to elastic deformations and formation of interstitial vortices. Hence, the question arises whether other arrangements—between the two extremes of periodic and random pinning arrangements—may lead to an enhanced vortex pinning over a broader range of applied magnetic field B.

Recently, it has been shown by numerical simulations[15,16] and experimentally[17–19] that a quasiperiodic arrangement of pinning sites produces additional commensurability effects and hence an enhanced pinning below the first matching field. A different proposal was made very recently by Reichhardt and Olson Reichhardt.[20] By molecular-dynamics simulations they investigated periodic pinning arrays that have been diluted by randomly removing the fraction P_d of pins, while keeping the pin density n_p fixed. Such arrays are very interesting, since with increasing dilution the pinning potential undergoes a gradual transition from periodic to purely random. Therefore, this model is suitable to explore the intermediate region between order and disorder, as it is usually found in real world. Interestingly, the simulations showed that the introduction of disorder leads to an enhanced critical current above the first matching field. In periodic pinning arrays the vortices sitting at the pinning sites form easy flow channels for interstitial vortices,[21] while for randomly diluted pinning arrays channeling should be suppressed.[20] This approach is also interesting from a general point of view, as the presence of disorder in competition with periodic potentials is also investigated in many other physical systems, e.g., two-dimensional conductors,[22] Ising ferromagnets,[23] and Josephson junction arrays.[24,25] For related recent work on vortex phases, see Ref. 26.

In this work, we present results on the experimental investigation of vortex pinning and flow in superconducting Nb thin films containing randomly diluted triangular arrays of submicron holes (antidots) as pinning sites. We studied $I_c(B)$ at variable temperature T close to the superconducting transition temperature T_c and we compare pinning arrays having different dilution, considering two different scenarios: (i) *Scaled lattices*. For different values of P_d, we fix the density n_p of pinning sites. Accordingly, the lattice parameter (smallest separation between pinning sites) scales as $a(P_d) = a(0)\sqrt{1-P_d}$. In this scenario a controlled transition from periodic to random arrangement of antidots is investigated. (ii) *Fixed lattices*. Here, we fix the lattice parameter a for different values of P_d. Accordingly, the density of pinning sites scales as $n_p(P_d) = (1-P_d)n_p(0)$. Here, with increasing P_d a transition to plain films (no antidots) is treated.

Our experimental results confirm essential features as predicted in Ref. 20. The fixed and scaled lattices show two different kinds of matching effects, which differently depend on temperature. Furthermore, the scaled lattices show an enhancement of I_c at magnetic fields above B_p with increasing dilution P_d. This effect is caused by suppression of vortex channeling and can be also observed in the dynamic regime, i.e., by measuring current-voltage (IV) characteristics.

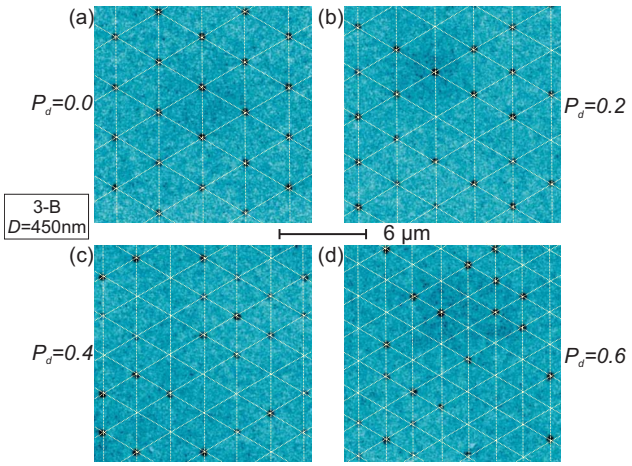

FIG. 1. (Color online) Scanning electron microscopy images of Nb thin films with randomly diluted antidot arrays; lines illustrate the triangular lattices. Lattice parameters $a(P_d)=3.4-2.1$ μm, for dilutions $P_d=0-0.6$, are scaled to maintain constant antidot density $n_p=0.1$ μm^{-2}.

II. SAMPLES

The experiments were carried out on $d=60$ nm thick Nb films which were deposited by dc magnetron sputtering in the same run on four separate Si substrates with 1 μm thick SiO_2 on top. Patterning was performed by *e*-beam lithography and lift off to produce Nb bridges of width $W=200$ μm and length $L=640$ μm. The bridges contain circular antidots (diameter $D=260-550$ nm) arranged in a triangular lattice that has been randomly diluted, with dilutions $P_d=0$ ("undiluted array"), 0.2, 0.4, 0.6, 0.8, and 1 ("plain" film, without antidots). Each chip (nos. 1–4) contains two or three sets (A, B, C) of bridges. Each set has six bridges with different values for $P_d=0-1$. The antidot diameter D is kept constant within each set and varies from set to set. Chips 1 and 2 contain sets of bridges with fixed lattice parameter $a=1.5$ μm, i.e., the density of vertices of the corresponding triangular lattice is $n_l=\frac{2}{\sqrt{3}}\frac{1}{a^2}=0.5$ μm^{-2}, which corresponds to the "lattice matching field" $B_l\equiv n_l\Phi_0=1.1$ mT (denoted as B_ϕ^* in Ref. 20). For those two chips, the antidot density n_p decreases from 0.5 to 0.1 μm^{-2} with increasing P_d from 0 to 0.8. Chips 3 and 4 contain sets of bridges with scaled lattice parameters $a(P_d)=3.4-1.5$ μm for $P_d=0$ to $P_d=0.8$, respectively, in order to have a fixed antidot density $n_p=0.1$ μm^{-2} and "pin density" matching field $B_p=0.21$ mT (denoted as B_ϕ in Ref. 20), with $N_p\approx 12\,500$ antidots in each bridge. Below we present results obtained on bridges from sets 1-B ($D=300$ nm), 3-B ($D=450$ nm), [c.f. Fig. 1], 4-B ($D=360$ nm), and 4-A ($D=260$ nm). A summary of the relevant sample parameters is given in Table I.

III. EXPERIMENTAL SETUP

For electric transport measurements, the samples are mounted in an evacuated chamber which is inserted into a glass fiber cryostat filled with liquid helium. The cryostat is surrounded by a three-layer magnetic shield and is placed in an rf-shielded room. A superconducting magnet allows to apply a well-controlled magnetic field. The sample is mounted together with a Si-diode temperature sensor on a sapphire substrate. Heating the backside of the sapphire substrate (covered by an absorbing layer) via a temperature-stabilized diode laser, the sample temperature can be adjusted from 4.2 up to 100 K. Using a temperature controller with a feedback loop to control the laser heating power, we achieve a temperature stability, measured at the Si diode, of about 1 mK. The setup allows to perform electric transport measurements on four bridges on a chip simultaneously.

TABLE I. Antidot diameter D, antidot density n_p, and vertex density $n_l\propto 1/a^2$ of the sets of bridges with randomly diluted antidot arrays used in this paper. Each set contains five bridges with different dilutions $P_d=0$ (undiluted array), 0.2, 0.4, 0.6, 0.8, and 1 (plain film, without antidots).

	D (nm)	n_p (μm^{-2})	n_l (μm^{-2})
1-B	300	$(1-P_d)0.5$	0.5 (fixed a)
3-B	450	0.1 (scaled a)	$0.5/(1-P_d)$
4-A	260	0.1 (scaled a)	$0.5/(1-P_d)$
4-B	360	0.1 (scaled a)	$0.5/(1-P_d)$

IV. RESULTS

To characterize our devices, we first measured resistance R vs T at $B=0$ and determined T_c and normal resistance $R_n\equiv R(T=10$ K) (with bias current $I=2$ μA) of the different bridges on each chip. Due to the strong influence of the reduced temperature $t\equiv T/T_c$ (for T close to T_c) on the characteristic length scales, i.e., the London penetration depth $\lambda(t)$ and coherence length $\xi(t)$, and on $I_c(t)$, the determination of T_c plays an important role for the comparison and interpretation of the performance of pinning arrays with different P_d. We defined T_c by linear extrapolation of the $R(T)$ curves in the transition region to $R=0$, i.e., T_c marks the onset of resistance. For all samples we find $T_c\approx 8.5$ K with a variation of a few mK within each set of bridges and $R_n=5.0-5.8$ Ω, depending on n_p and D. Within the sets ($D=const$) with $n_p=const$ (scaled lattices), R_n varies by less than $\pm 2\%$ from bridge to bridge. The plain film (from set 4-A) has $R_n=5.0$ Ω, which yields a normal resistivity $\rho_n=R_n dW/L=9.4$ $\mu\Omega$ cm. With the relation $\rho\ell=3.72\times 10^{-6}$ $\mu\Omega$ cm^2,[27] we estimate for the mean-free path $\ell=4.0$ nm. All I_c values were determined with a voltage criterion $V_c=1$ μV.

A. Commensurability effects in randomly diluted triangular arrays

Figure 2 shows $I_c(B/B_p)$ patterns of four randomly diluted bridges with similar antidot size at various temperatures $t=T/T_c=0.9995-0.9965$. I_c was normalized to its maximum value at $B=0$. Two bridges (from set 4-A) have the same antidot density $n_p=0.1$ μm^{-2} and dilution $P_d=0.2$ (a) and $P_d=0.4$ (c). The two other bridges (from set 1-B) have larger

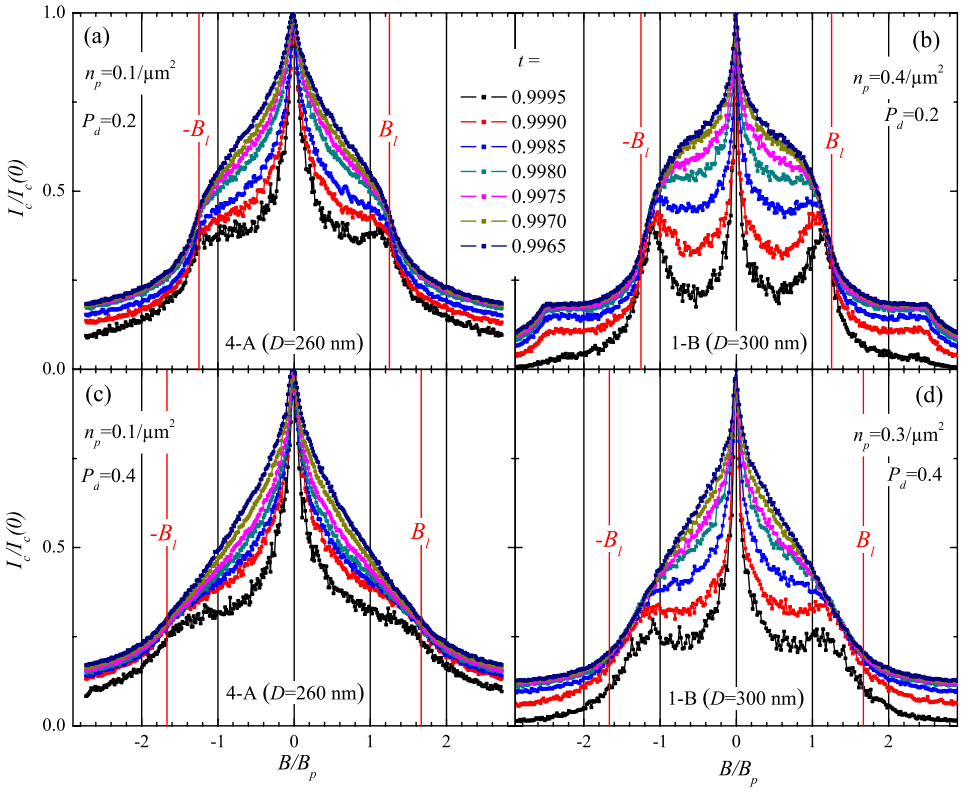

FIG. 2. (Color online) (Double column) $I_c/I_c(0)$ vs B/B_p for randomly diluted arrays at different reduced temperatures (I_c increases with decreasing t). Comparison of the dependence on the antidot density n_p for samples with [(a) and (b)] P_d=0.2 and [(c) and (d)] P_d=0.4.

antidot densities n_p=0.4 μm^{-2} with P_d=0.2 (b) and n_p =0.3 μm^{-2} with P_d=0.4 (d). The applied field is always normalized to $B_p \propto n_p$.

For the highest t=0.9995, a clear peak in $I_c(B)$ indicates matching of the vortex lattice with the pinning array, as shown in Fig. 2(b). The position of the peak is located between B_p and B_l. This indicates that indeed "pin density matching" is observed; however, as pointed out in Ref. 20, for a diluted periodic pinning array at $B=B_p$, the vortex configuration contains numerous topological defects. Hence, commensurability effects at B_p can only be observed when pinning is so strong that the lattice distortion energy, associated with the deviation from an ideal triangular vortex lattice, can be overcome. This is most likely to be observed for the samples with higher density of pinning sites. Accordingly, for a given P_d, the matching peak is more pronounced in the samples with 3 and 4 times larger n_p, as shown in Fig. 2 by comparison of graphs (a) and (b) for P_d=0.2 and by comparison of graphs (c) and (d) for P_d=0.4.

With decreasing n_p and t and with increasing P_d, the peak in $I_c(B)$ gradually transforms into a shoulderlike structure, located close to B_p. Following the evolution of $I_c(B)$ with decreasing temperature shows that $I_c(B<B_p)/I_c(0)$ increases most whereas $I_c(B_l)/I_c(0)$ is almost independent of t. For the larger P_d=0.4, this leads gradually to a transformation of the shoulderlike structure into a triangular-shaped $I_c(B)$ pattern without any indication of matching effects, either at B_p or B_l. Nevertheless, I_c for P_d=0.4 is still significantly enhanced over I_c for samples without antidots, as will be shown below.

B. Different dilution

In the following, we directly compare pinning arrays having different dilutions P_d at the same reduced temperature.

1. Fixed lattice parameter—transition to plain

Figure 3 shows $I_c(B)$ patterns of samples with fixed lattice parameter a=1.5 μm (n_l=0.5 μm^{-2}) at t=0.9990 (a) and t =0.9965 (b). The B axis is normalized to the lattice matching field B_l, which is the same for all perforated bridges within this set. The sample with P_d=0 shows pronounced peaks in $I_c(B)$ which are located at $\pm B_l$ and $\pm 2B_l$, indicating a saturation number $n_s \geq 2$ (Refs. 28 and 29) for both temperatures.

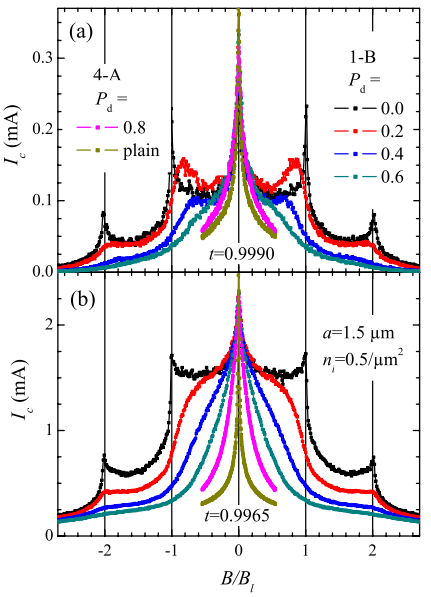

FIG. 3. (Color online) I_c vs B/B_l at (a) t=0.9990 and (b) 0.9965 for arrays with fixed lattice parameter a and variable dilution P_d. $I_c(B>B_l)$ decreases with increasing P_d.

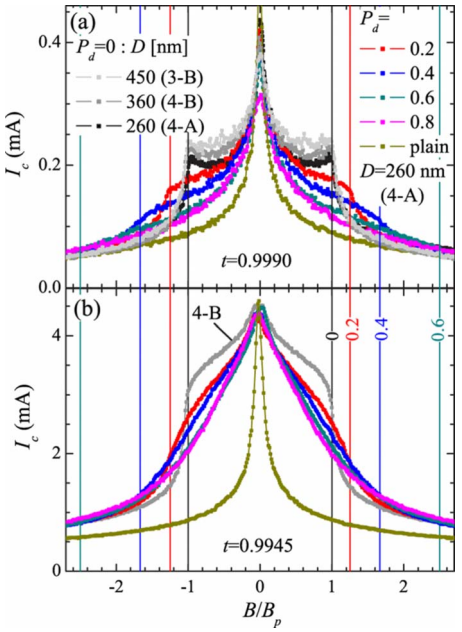

FIG. 4. (Color online) I_c vs B/B_p at (a) $t=0.9990$ and (b) 0.9945 for arrays with scaled lattice parameters $a(P_d)$ (fixed antidot density $n_p=0.1\ \mu\text{m}^{-2}$ and matching field B_p). Comparison of samples having different dilutions P_d and different antidot diameters D for $P_d=0$. $I_c(B \lesssim B_p)$ decreases with decreasing D (for $P_d=0$) and with increasing P_d. Vertical solid lines indicate $\pm B_l(P_d)/B_p$, labeled with corresponding values for P_d.

In the samples with small dilution ($P_d=0.2$ and 0.4) we also find peaks in $I_c(B)$ for the higher temperature shown in Fig. 3(a). The matching peaks are significantly broader than the matching peaks of the undiluted bridge and they are located at magnetic fields between B_l and $B_p(P_d)$. This is also visible in Figs. 2(b) and 2(d). With increasing P_d we find a gradual transition of the $I_c(B)$ patterns at $B<B_l$ from the undiluted array ($P_d=0$) to the plain film ($P_d=1$). As predicted in Ref. 20, for fixed lattices an increase in P_d generally results in a decrease of I_c (for all values of applied field $B \neq 0$), as expected for the gradual transition from a periodic pinning array to a plain film without antidots. However, we would like to mention one exception, which we observed for the highest temperature. For $t=0.9990$ [c.f., Fig. 3(a)] the diluted sample with $P_d=0.2$ shows a higher I_c than the undiluted sample ($P_d=0$) for $B<B_l$ and very similar I_c values for all other fields, except for the matching fields B_l and $2B_l$. This effect is quite counterintuitive, as it means that simply by removing 20% of the antidots (without rescaling the antidot distance and density), I_c can be increased for fields below B_l. This effect has not been predicted in Ref. 20 and is probably due to a subtle interplay between pinning energy and elastic energy of the vortex lattice, which may lead to a transition from plastic to elastic depinning for this special case.

2. Scaled lattice parameter—transition to random

Figure 4 shows $I_c(B/B_p)$ patterns of bridges with scaled lattice parameters $a(P_d)$, i.e., $n_p=const$, with different $P_d=0-1$ at $t=0.9990$ (a) and $t=0.9945$ (b). In Fig. 4(a) data from set 4-A ($D=260$ nm) are complemented by results from two undiluted bridges with $D=360$ nm (4-B) and $D=450$ nm (3-B) in order to demonstrate the effect of antidot size. All bridges with $P_d=0$ and different D show qualitatively the same $I_c(B)$ patterns. The major difference is a slight increase in I_c at $B<B_p$ with increasing D. This dependence can be explained with the increase of the pinning strength of the antidots with increasing D. For $B<B_p$, each vortex can be captured by an antidot and hence the increasing pinning strength with D leads to an increase of I_c. In contrast, for $B>B_p$, vortices occupy interstitial pinning sites where they are weakly pinned. Hence, I_c is drastically reduced and determined by the motion of interstitial vortices, which should not depend on the antidot size. This is exactly what we find experimentally, i.e., $I_c(B>B_p)$ is independent of D for the samples with $P_d=0$.

With increasing P_d (decreasing a in order to keep the antidot density n_p constant) the shape of the $I_c(B/B_p)$ patterns is strongly affected. The diluted arrays show "lattice matching" effects around B_l. It is interesting to note that with decreasing t the matching effects become less pronounced and the $I_c(B)$ pattern approaches more and more a triangular shape. This shape is reminiscent of the $I_c(B)$ pattern of randomly arranged antidots.[18] This can be understood as with increasing P_d and fixed n_p, the antidot arrangement approaches that of a random arrangement.

3. Suppression of channeling

For $P_d=0$ from set 4-A we have no data for the full range of t, as the bridge was damaged after taking first data. Hence, to facilitate the comparison of different P_d at $t=0.9945$ [Fig. 4(b)], we also show data from another bridge with $P_d=0$ (from set 4-B). For both temperatures ($t=0.9990$ and $t=0.9945$) we find a decrease in I_c with increasing P_d for $B<B_p$. However, for $B>B_p$ the diluted arrays show an enhanced I_c as compared to the undiluted sample(s). Both observations are in qualitative agreement with the simulations in Ref. 20. We do find that the enhancement of I_c above B_p persists up to the highest dilution $P_d=0.8$. This enhancement was explained in Ref. 20 with the suppression of channeling of interstitial vortices for fields in the range $B_l<B<B_p$. For undiluted arrays, this channeling effect causes the rapid decrease of I_c with increasing B slightly above B_p [c.f. Fig. 4]. Our experimental data clearly confirm that this rapid drop in I_c at B_p is absent for the diluted arrays.

The suppression of channeling should also be visible in the current-voltage characteristics. Figure 5(a) shows the $V(I)$ curves of differently diluted samples at $B=2B_p$ and $t=0.9945$, and Fig. 5(b) shows the corresponding differential resistance dV/dI vs current curves. The $V(I)$ curves directly correspond to the $I_c(B)$ pattern shown in Fig. 4(b). For Fig. 5 we have chosen values of t and B for which I_c is essentially the same for all values of P_d (except for $P_d=1$) in order to facilitate the comparison for different values of P_d regarding the evolution of the flux-flow voltage with increasing current. For the undiluted bridge at $B=2B_p$ one expects the same number of vortices sitting in the antidots and at interstitial positions. In this case we find two critical depinning currents $I_{c,1}$, $I_{c,2}$ in the $V(I)$ curves [c.f. inset of Fig. 5(b)]. $I_{c,1} \approx 1$ mA corresponds to the current above which a finite

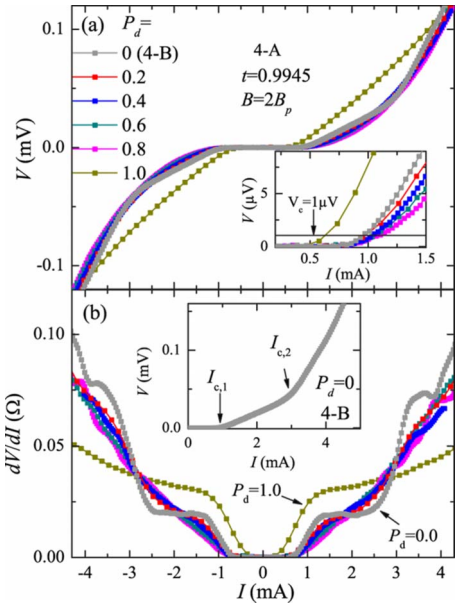

FIG. 5. (Color online) (a) $V(I)$ curves and (b) $dV/dI(I)$ curves at $B=2B_p$ and $t=0.9945$ for arrays with scaled lattice parameters $a(P_d)$ (fixed antidot density $n_p=0.1$ μm^{-2} and matching field B_p). Inset in (a) shows magnification of V vs I at small voltages; $V(I>1$ mA) decreases with increasing P_d, except for the plain film ($P_d=1$) with lowest I_c. Inset in (b) shows V vs I for $P_d=0$ only with the critical depinning current $I_{c,1}(I_{c,2})$ of interstitial (pinned) vortices.

voltage appears. This voltage is caused by the motion of weakly pinned interstitials. At a higher current $I_{c,2}\approx 3$ mA the slope of the IV curve changes. This is due to the depinning of vortices sitting in the antidots. The value of $I_{c,2}$ can also be found in the $I_c(B)$ pattern shown in Fig. 4(b). $I_{c,2}$ fits quite well to the critical current at the first matching field $I_c(B_p)$. The $dV/dI(I)$ curves in Fig. 5(b) reveal some further features, which are not easily visible in the $V(I)$ curves shown in Fig. 5(a). The undiluted sample ($P_d=0$) shows a sharp increase in dV/dI at $I_{c,1}$, followed by an almost constant $dV/dI\approx 18$ mΩ. For the diluted arrays, this steplike change in dV/dI gets smeared out, and with increasing P_d the $dV/dI(I)$ curves become increasingly smooth. The undiluted sample shows another steplike increase in $dV/dI(I)$ at $I_{c,2}$, followed by another plateau at ≈72 mΩ, i.e., a factor of 4 above the first plateau. Finally, a third steep increase in dV/dI sets in at $I\approx 3.9$ mA. This value of bias current seems to coincide with the value of $I_c(B\approx 0.2B_p)$ at which the initial steep decrease in $I_c(B)$ (with increasing B) for the undiluted sample transforms into the broad domelike structure, as shown in Fig. 4(b). Currently, we cannot explain this feature. Finally we note that all diluted samples ($P_d=0.2-0.8$) have a similar $I_{c,1}$ but do not show a pronounced dV/dI change at $I_{c,2}$. The inset in Fig. 5(a) clearly shows that with increasing P_d the voltage due to flux motion decreases, i.e., in the diluted pinning arrays dissipation is reduced, due to the more effective suppression of vortex channeling.

V. CONCLUSIONS

In conclusion, we experimentally investigated Nb thin films with triangular arrays of antidots, which have been randomly diluted, by measurements of the critical current I_c vs applied magnetic field B and current-voltage (IV) characteristics close to the transition temperature T_c. The antidot lattices could be tuned to find two different matching effects, related to the antidot density and to the lattice parameter of the antidot lattice, as predicted in Ref. 20. For samples with fixed lattice parameter, with increasing dilution P_d a gradual transition from a periodic pinning array to a plain film without pinning sites has been observed. Obviously, with increasing P_d the critical current decreases. However, very close to T_c, for small dilutions ($P_d=0.2$) we do find a broad peak in $I_c(B)$ located between B_p and B_1, corresponding to an increase in I_c by removing 20% of the pinning sites. We speculate that this counterintuitive effect is due to the introduction of disorder; an understanding of this effect is still lacking and deserves further investigations. On the other hand, for samples with fixed antidot density, an increasing dilution corresponds to a gradual transition from a periodic to purely random distribution of pinning sites. Our experiments clearly show an enhancement of I_c for magnetic fields above B_p with increasing P_d. This was the main prediction in Ref. 20 and can be explained with the suppression of channeling of interstitial vortices. This effect is also observed in IV measurements, i.e., the suppression of channeling causes an increasing reduction in the flux-flow voltage with increasing P_d. As a consequence, the concept of introducing disorder by randomly removing pinning sites in tailored periodic pinning arrays seems to provide a feasible way for enhancing the critical current in superconductors for magnetic fields above the matching field B_p.

ACKNOWLEDGMENTS

This work was supported by the DFG via the SFB/TRR21 and in part by the DFG Research Center of Functional Nanostructures. M.K. gratefully acknowledges support from the Carl-Zeiss-Stiftung.

*kemmler@pit.physik.uni-tuebingen.de

[1] P. T. Korda, M. B. Taylor, and D. G. Grier, Phys. Rev. Lett. **89**, 128301 (2002).
[2] D. J. Pine, J. P. Gollub, J. F. Brady, and A. M. Leshansky, Nature (London) **438**, 997 (2005).
[3] E. Y. Andrei, G. Deville, D. C. Glattli, F. I. B. Williams, E. Paris, and B. Etienne, Phys. Rev. Lett. **60**, 2765 (1988).
[4] G. Grüner, Rev. Mod. Phys. **60**, 1129 (1988).
[5] M. O. Magnasco, Phys. Rev. Lett. **71**, 1477 (1993).
[6] P. Reimann, Phys. Rep. **361**, 57 (2002).
[7] P. Hänggi, F. Marchesoni, and F. Nori, Ann. Phys. **14**, 51 (2005).
[8] V. V. Moshchalkov, V. Bruyndoncx, L. Van Look, M. J. Van

Bael, Y. Bruynseraede, and A. Tonomura, in *Handbook of Nanostructured Materials and Nanotechnology: Electrical Properties*, edited by H. S. Nalwa (Academic, New York, 2000), Vol. 3, p. 451.
[9] O. Daldini, P. Martinoli, J. L. Olsen, and G. Berner, Phys. Rev. Lett. **32**, 218 (1974).
[10] A. T. Fiory, A. F. Hebard, and S. Somekh, Appl. Phys. Lett. **32**, 73 (1978).
[11] M. Baert, V. V. Metlushko, R. Jonckheere, V. V. Moshchalkov, and Y. Bruynseraede, Phys. Rev. Lett. **74**, 3269 (1995).
[12] J. I. Martin, M. Velez, J. Nogues, and I. K. Schuller, Phys. Rev. Lett. **79**, 1929 (1997).
[13] M. J. Van Bael, K. Temst, V. V. Moshchalkov, and Y. Bruynseraede, Phys. Rev. B **59**, 14674 (1999).
[14] J. E. Villegas, E. M. Gonzalez, M. I. Montero, I. K. Schuller, and J. L. Vicent, Phys. Rev. B **68**, 224504 (2003).
[15] V. Misko, S. Savel'ev, and F. Nori, Phys. Rev. Lett. **95**, 177007 (2005).
[16] V. R. Misko, S. Savel'ev, and F. Nori, Phys. Rev. B **74**, 024522 (2006).
[17] J. E. Villegas, M. I. Montero, C.-P. Li, and I. K. Schuller, Phys. Rev. Lett. **97**, 027002 (2006).
[18] M. Kemmler, C. Gürlich, A. Sterck, H. Pöhler, M. Neuhaus, M. Siegel, R. Kleiner, and D. Koelle, Phys. Rev. Lett. **97**, 147003 (2006).
[19] A. V. Silhanek, W. Gillijns, V. V. Moshchalkov, B. Y. Zhu, J. Moonens, and L. H. A. Leunissen, Appl. Phys. Lett. **89**, 152507 (2006).
[20] C. Reichhardt and C. J. Olson Reichhardt, Phys. Rev. B **76**, 094512 (2007).
[21] M. Velez, D. Jaque, J. I. Martin, M. I. Montero, I. K. Schuller, and J. L. Vicent, Phys. Rev. B **65**, 104511 (2002).
[22] A. Dorn, E. Bieri, T. Ihn, K. Ensslin, D. D. Driscoll, and A. C. Gossard, Phys. Rev. B **71**, 035343 (2005).
[23] R. B. Griffiths, Phys. Rev. Lett. **23**, 17 (1969).
[24] Y.-H. Li and S. Teitel, Phys. Rev. Lett. **67**, 2894 (1991).
[25] E. Granato and D. Domínguez, Phys. Rev. B **63**, 094507 (2001).
[26] W. V. Pogosov, V. R. Misko, H. J. Zhao, and F. M. Peeters, Phys. Rev. B **79**, 014504 (2009).
[27] A. F. Mayadas, R. B. Laibowitz, and J. J. Cuomo, J. Appl. Phys. **43**, 1287 (1972).
[28] G. S. Mkrtchyan and V. V. Schmidt, Sov. Phys. JETP **34**, 195 (1972).
[29] G. R. Berdiyorov, M. V. Milosevic, and F. M. Peeters, Phys. Rev. B **74**, 174512 (2006).